Morphological and optical variations induced by p-n dopants in $Ga_xIn_{(1-x)}P$ nanowires homojunctions monolithically integrated on Si (111) for photovoltaic applications

Bologna, N.[1,2,3], Wirths, S.[2], Francaviglia, L.[3], Campanini, M.[1], Schmid, H.[2], Theofylaktopoulos, V.[2], Moselund, K.[2], Fontcuberta i Morral, A.[3], Erni, R.[1], Riel, H.[2] and D. Rossell, M.[1]

[1] Empa, Swiss Federal Laboratories for Materials Science and Technology, Dübendorf, Switzerland, [2] IBM Research-Zurich, Rüschlikon, Switzerland, [3] École Polytechnique Fédérale de Lausanne, Lausanne, Switzerland

III-V semiconductor nanowires (NWs) attracted significant research interest in recent years due to their superior physical properties and their potential applications in novel nanodevices [1]. In addition, their large surface-to-volume ratio holds the promise to realize new high-performance photovoltaic devices, in particular related to intentionally doped $Ga_xIn_{(1-x)}P$ NWs which can perfectly fit the requirements for nano-tandem solar cells [2]. However, the high-quality catalyst-free integration on Si and the influence of dopants on morphology and properties need to be further addressed prior to their implementation in real devices.

In this work, we present a thorough investigation of zincblende $Ga_xIn_{(1-x)}P$ NWs homojunctions that are for the first time monolithically integrated on (111)-oriented Si substrates using template-assisted selective epitaxy (TASE). TASE allows growing shape- and size-controlled nanostructures by means of a silicon oxide nanotube template without the use of any catalysts particle (Fig.1a) [3]. Furthermore, by means of STEM techniques, we have investigated the variations induced by the Si and Zn dopants on the crystal morphology, composition and optical properties of the NWs. While the undoped structures, analyzed by EDX spectroscopy, were found to be compositionally homogeneous along the entire length (Fig. 1c,d,e), the n- and p-segments of the doped $Ga_xIn_{(1-x)}P$ NWs (with a nominal doping of $1.5x10^{19}$ cm^{-3}) show an increase of the In and Ga content (Fig.2), respectively. Furthermore, the p-segment showed a net decrease in the defects density. Accordingly, low-loss EELS reveals a blue shift (+0.6 eV) of the bulk plasmon peak associated with the material inhomogeneities (Fig. 3b). Finally, the optical properties of the p-n junction were verified by cathodoluminescence (CL), showing a variation in the peak of the emission spectra from 1.73 eV to 1.93 eV for the n- and p-type region (Fig. 3c), respectively, while the interface shows a dominant emission at 1.98 eV. Band gap simulations reproducing the p-n junction suggest that the emission originates from the donor and acceptor levels in the bandgap induced by the relatively high doping concentrations. On the contrary, at the depletion region, these levels are already occupied, allowing the exciton recombination to happen between the top of the valence band and the bottom of the conduction band.

In conclusion, a detailed investigation focused on the effects induced by p-n dopants on morphology, composition and optical properties of vertical $Ga_xIn_{(1-x)}P$ NWs homojunctions succesfully integrated for the first time on Si (111) by TASE technique was performed. We consider these results to open new possibilities in the catalyst-free implementation of $Ga_xIn_{(1-x)}P$ NWs on Si for the realization of nano-tandem solar cells.

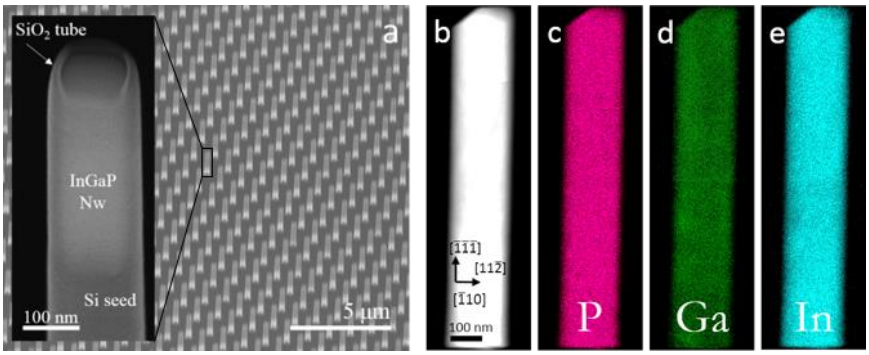

Fig. 1: (a) SEM image showing a region of InGaP NWs grown on Si(111). (b) HAADF and EDX maps of (c) phosphorous, (c) gallium and (d) indium content in undoped $Ga_xIn_{(1-x)}P$ NWs.

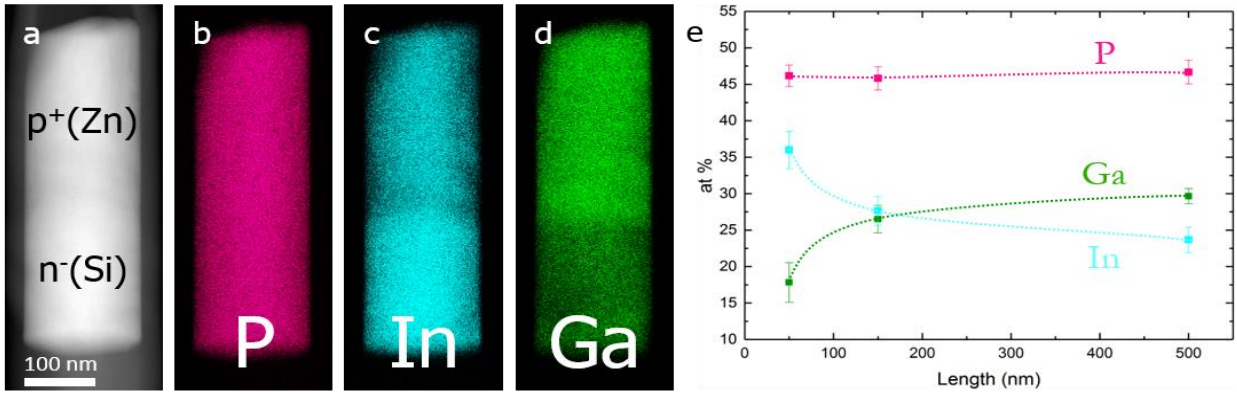

Fig. 2: (a) HAADF micrograph and corresponding EDX chemical maps showing the (b) phosphorous, (c) gallium and (d) indium content in doped $Ga_xIn_{(1-x)}P$ NWs. (e) Compositional trend averaged on six different NWs at three different distances from the interface with the silicon at the bottom of the NW.

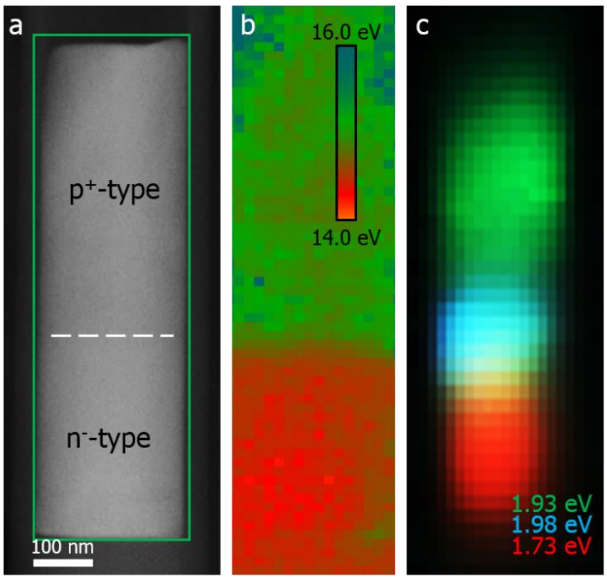

Fig. 3: (a) HAADF micrograph of a doped $Ga_xIn_{(1-x)}P$ NW and corresponding (b) EELS bulk plasmon map and (c) CL map acquired in the green box showing how in both cases an energy shift from the n- to the p-segment occurs.

[1] A. M. Ionescu et al, Nature **479**, 329 (2011).

[2] Y. Özen et al, Sol. Energy Mater. Sol. Cells **137**, 1 (2015).

[3] M. Borg et al, J. Appl. Phys. **117**, 144303 (2015).

[4] This project was financially supported by the European Union H2020 program Nano-Tandem (Grant Agreement No. 641023) and the Swiss National Science Foundation (project no. 200021_156746 200021_169908 through the NCCR QSIT).